DOI: 10.1002/ejic.200500698

Structural, Electrochemical, and Theoretical Investigations of New Thio- and Selenoether Complexes of Molybdenum and Tungsten

Xiaoli Ma,[a] Kerstin Starke,[a] Carola Schulzke,*[a] Hans-Georg Schmidt,[a] and Mathias Noltemeyer[a]

Keywords: Bioinorganic chemistry / Molybdenum / Tungsten / Ligand effects / Redox chemistry

Molybdenum and tungsten complexes with tridentate bis-anionic ligands ($^{-}OC_2H_4XC_2H_4O^{-}$, X = S, Se) were synthesized and analyzed electrochemically. Crystal structures of $[\{MoO_2[O(CH_2)_2S(CH_2)_2O]\}_2]$ and $[\{WO_2[O(CH_2)_2S(CH_2)_2O]\}_3]$ were obtained. For these two complexes as well as for the virtual molybdenum trimer and the tungsten dimer, DFT calculations were performed in order to better understand the formation of two significantly different complexes for molybdenum and tungsten with the same ligand and by the same preparation method. The compound $WO_2Cl_2[MeS(CH_2)_2SMe]$ was synthesized and characterized by crystal structure analysis. A structural and electrochemical comparison of this compound with the recently published analogous molybdenum compound and the dme analogs of molybdenum and tungsten were undertaken. All these data were used to evaluate the structural and electronic influences of replacing molybdenum by tungsten and of varying the ligand atoms (O/S/Se) from the point of view of the different coordination spheres of the molybdopterin-dependent oxygen-atom-transfer enzymes.

Introduction

Molybdenum as well as tungsten can be found at the active sites of the molybdopterin-containing oxygen-atom-transfer enzymes (OATs),[1] which catalyze oxygen transfer by two-electron redox reactions. This is not surprising because of the chemical similarity of the two metals. The distribution of the metals is quite interesting; molybdenum is found mainly in mesophilic organisms while tungsten is found mainly in thermophilic and hyperthermophilic microorganisms, and it is not known until today whether this distribution was developed for reasons of supply,[2,3] stability,[2,4] or reactivity[5] (i.e. redox potential). Therefore, the comparison of the characteristics of corresponding molybdenum and tungsten compounds remains a vital field of research.

Another interesting diversity of these enzymes is that, in the DMSO reductase family[6] (molybdenum enzymes with two molybdopterin ligands), the metal is bound to the peptide moiety through either serine (O),[7] cysteine (S),[8] selenocysteine (Se),[9] or aspartate (O, mono- or bidentate).[10] The amino acid ligands are supposed to play a role in stabilizing the enzyme–substrate complexes. It is still not known whether the different types of amino acid ligands are used purposefully or merely accidentally. The coordination of selenocysteine as well as the coordination of sulfur atoms to tungsten were also established, although far fewer structures of tungsten-containing OATs are available.[11,12]

High-valent metal complexes with thioether or selenoether ligands that represent hard–soft metal–ligand combinations are relatively rare mainly because these compounds are rather unstable.[13]

Even though molybdenum(VI) and tungsten(VI) can be considered as moderately hard, only a handful of thioether or selenoether complexes of these metals are known.[14–17]

In spite of the assumption that these kinds of complexes with Mo^{VI} and W^{VI} may not be easy to prepare and handle, we tried to synthesize and characterize a small variety of these compounds with additional alkoxy functions at the ligands for enhanced stability. In the synthesis we focused on the simple replacement of acetylacetonate ligands in $MO_2(acac)_2$ (M = Mo, W) by alkali salts of alkoxylates containing a thio- or selenoether function. We had two reasons for this: (i) In this way we would obtain complexes that mimic the active sites of the OATs where the coordination sphere of the metal consists only of oxygen and sulfur or selenium, respectively, and where one oxo ligand is present with an oxidation state of +6 for the metal. (ii) We would also obtain complexes that enable us to compare the influences of molybdenum versus tungsten and sulfur versus selenium with regard to their redox properties. Although in the enzymes the sulfur atom is bound as the thiolate or sulfido ligand and the selenium as the selenate ligand, the investigation of the ether variants of these ligand atoms could give some insight into their influence. The focus here

[a] Institut f. Anorganische Chemie, Universität Göttingen, Tammannstr. 4, 37077 Göttingen, Germany
Fax: +49-551-393373
E-mail: carola.schulzke@chem.uni-goettingen.de
Supporting information for this article is available on the WWW under http://www.eurjic.org or from the author.

was to evaluate atom-dependent structural and redox potential changes that might offer a clue as to whether the different types of OATs having different coordinated amino acids, were developed for fine tuning of the redox potential, for their structural influence, or just by chance.

We also synthesized the compound $WO_2Cl_2[MeS(CH_2)_2SMe]$, which is analogous to a recently published molybdenum compound.[14] The compounds $MO_2Cl_2(dme)$ are well-established for both metals.[18,19] Therefore, with this new compound a thorough structural and electrochemical investigation of these compounds and a comparison between oxygen and sulfur coordination as well as a comparison between molybdenum and tungsten compounds could be undertaken. The results are presented here.

Results and Discussion

Synthesis and Structural Analysis

$WO_2Cl_2[MeS(CH_2)_2SMe]$ (**1**) was synthesized by an analogous method to the published preparation of $MoO_2Cl_2[MeS(CH_2)_2SMe]$[14] (Scheme 1). The starting material (WO_2Cl_2) was prepared in situ from $WOCl_4$.

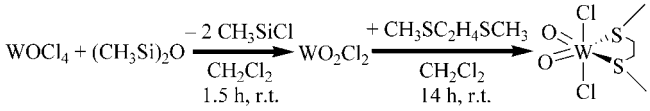

Scheme 1. Preparation of $WO_2Cl_2(CH_3SC_2H_4SCH_3)$ (**1**).

The structures of $MoO_2Cl_2[MeS(CH_2)_2SMe]$[14] and $WO_2Cl_2[MeS(CH_2)_2SMe]$ (**1**) (see Figure 1) are almost identical, and the largest differences occur for the metal–chlorine bond length (0.05 Å) and the O=M=O angle (1°) (see Table 1). Both compounds crystallize in the same crystal system (hexagonal) and space group ($P6_1$).

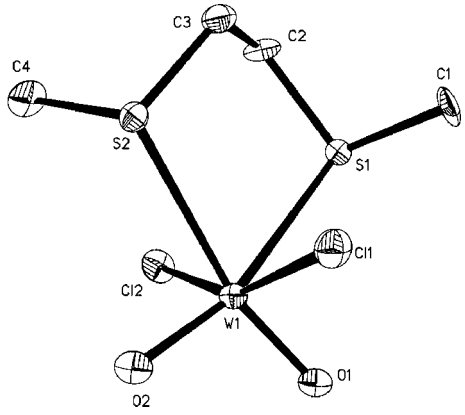

Figure 1. View of the structure of $WO_2Cl_2[MeS(CH_2)_2SMe]$ (**1**) (with numbering Scheme). Hydrogen atoms are not shown. Ellipsoids are drawn at 50% probability.

This is also true for the compounds $MoO_2Cl_2(dme)$[18] and $WO_2Cl_2(dme)$,[19] where the largest difference for a bond length is that for the M–O(ether) bond of 0.04 Å, and the difference for the O(ether)–M–O(ether) angle is 0.4°, which is the largest difference for an angle. Nevertheless, it has to be noted that the value for the Cl–Mo–Cl angle is not mentioned in the respective publication.[18] Again, both compounds crystallize in the same crystal system (monoclinic) and space group ($P2_1/n$).

The differences observed as a result of a comparison of ether and thioether ligands are of course larger, but only for those values that are derived directly from the different radii of the oxygen and sulfur atoms. The difference in the metal–ether/thioether bond is 0.49 Å for the molybdenum complexes and 0.50 Å for the tungsten complexes. The values for the O/S–M–O/S angles differ by 6.5° for the molybdenum and by 6.9° for the tungsten compound, where the angles for the thioether ligands are wider. All other distances and angles involving the metal center are only slightly influenced; the largest difference for a bond length was 0.05 Å for the Mo–Cl bond and the largest difference for an angle was 2.5° for the Cl–W–Cl angle.

This is an indication that the electronic influence of replacing oxygen ligand atoms by sulfur ligand atoms is only very small. Otherwise we would have observed larger differences, especially in the parameters for the ligand atoms that are in a *trans* position to the ether/thioether functions (oxo ligands in all four cases).

The compounds $[\{MoO_2[O(CH_2)_2S(CH_2)_2O]\}_2]$ (**2**), $[\{WO_2[O(CH_2)_2S(CH_2)_2O]\}_3]$ (**3**), and $[\{WO_2[O(CH_2)_2Se(CH_2)_2O]\}_n]$ (**4**) were all prepared by the same method (Scheme 2). The ligand and the $MO_2(acac)_2$ precursor were combined in a CH_2Cl_2 solution, stirred at room temperature for one to two days, and filtered. The compounds were isolated from the filtrate by crystallization or drying in vacuo. The yields range from a rather good 60% for the tungsten selenoether (**4**) compound (obtained by drying) to only 32% for the tungsten thioether compound (**3**). Because we were unable to obtain crystals of the tungsten selenium compound, ^{77}Se NMR spectroscopy was performed on the complex (δ = 100.22 ppm) as well as on the ligand (δ = 68.23 ppm), in addition to the usual characterization methods. In both spectra, we observed only one signal that was shifted to higher frequencies/lower field in the complex, which indicates that a metal–selenium bond was indeed formed.[20]

Suitable crystals of the molybdenum and tungsten thioether compounds were analyzed by X-ray crystallography with quite interesting results (see Figure 2 and Figure 3).

The molybdenum complex with the thioether ligand has a dimeric structure in which the two molybdenum atoms are bridged by one alkoxylate function of each of the two thioether ligands. The tungsten, on the other hand, forms a trimeric structure in which one of the former oxo ligands of each metal bridges two tungsten atoms, forming a six-membered ring. In both structures, the metal achieves a slightly distorted octahedral coordination geometry through the two different kinds of aggregation, although the molybdenum is explicitly only bound to five ligand atoms with rather long metal–sulfur distances. Instead of the usual distance between the metal (molybdenum or tungsten) and sulfur atoms of a thioether ligand, which is in the range of 2.45 to 2.77 Å,[14,21] we found distances of 2.93

Table 1. Selected bond lengths and angles for the molybdenum and tungsten complexes with bidentate ether and thioether ligands.

	$WO_2Cl_2(MeSC_2H_4SMe)$ (**1**)	$MoO_2Cl_2(MeSC_2H_4SMe)$[a]	$WO_2Cl_2(dme)$[b]	$MoO_2Cl_2(dme)$[c]
M=O [Å]	1.716	1.691	1.690	1.667
	1.716	1.699	1.690	1.673
M–Cl [Å]	2.333	2.345	2.344	2.347
	2.337	2.385	2.344	2.340
M–O/S [Å]	2.748	2.759	2.253	2.289
	2.752	2.771	2.292	2.281
O=M=O [°]	105.3	106.3	105.1	105.0
O/S–M–O/S [°]	77.4	77.3	70.5	70.9
Cl–M–Cl [°]	155.1	154.4	157.6	–

[a] Ref.[14] [b] Ref.[19] [c] Ref.[18]

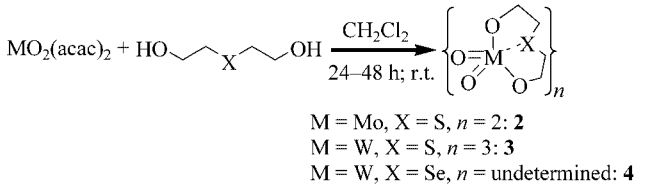

M = Mo, X = S, *n* = 2: **2**
M = W, X = S, *n* = 3: **3**
M = W, X = Se, *n* = undetermined: **4**

Scheme 2. Preparation of $[\{MoO_2[O(CH_2)_2S(CH_2)_2O]\}_2]$ (**2**), $[\{WO_2[O(CH_2)_2S(CH_2)_2O]\}_3]$ (**3**), and $[\{WO_2[O(CH_2)_2Se(CH_2)_2O]\}_n]$ (**4**). No X-ray structural analysis was possible for **4** and *n* could not be determined.

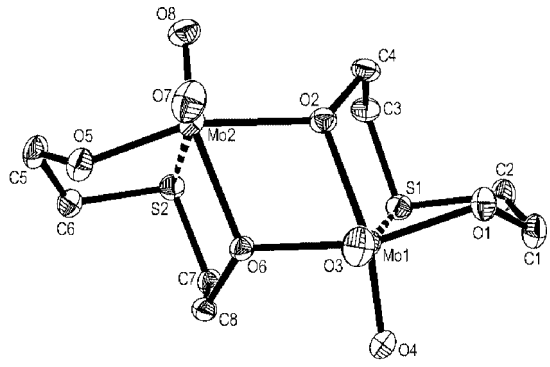

Figure 2. View of the structure of $[\{MoO_2[O(CH_2)_2S(CH_2)_2O]\}_2]$ (**2**) (with numbering scheme). Hydrogen atoms are not shown. Ellipsoids are drawn at 50% probability.

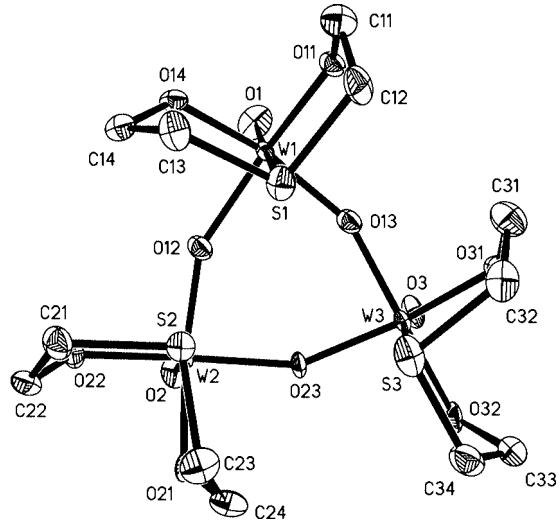

Figure 3. View of the structure of $[\{WO_2[O(CH_2)_2S(CH_2)_2O]\}_3]\cdot CH_2Cl_2$ (**3**·CH_2Cl_2) (with numbering scheme). Hydrogen atoms and solvent are not shown. Ellipsoids are drawn at 50% probability.

and 3.00 Å, indicating only weak bonds, if bonds at all. The tungsten–sulfur distances are shorter (2.79, 2.81, and 2.83 Å), even though the central metal is slightly larger, and these interactions can be considered bonds.

In spite of the fact that five-ring complexes with thio- or selenoether functions are supposed to be stable,[14] the expected molybdenum–sulfur bond with this ligand is not explicitly formed. The reaction of the OSO ligand with $MoO_2(acac)_2$ results in a compound that instead of forming two stable five-ring units, somehow rather resembles an eight-ring complex. In contrast, a certain monomeric molybdenum complex with the analogous ligand that contains an ether function instead of the thioether function is known to exhibit an oxygen(ether)–metal bond even though the distance is longer than usual.[22] This is not completely surprising for these kinds of ligands although the analogous cobalt complexes, with ligands where the alkoxylate and the ether/thioether functions are bridged by phenyl rings, show the reverse behavior. With the ether function, no bond is formed between the metal and oxygen atoms, whereas with the thioether function, there is a bond between the cobalt and sulfur atoms.[23]

Unfortunately, the crystals of **3** were racemic twins, and the structure could only be solved in an acentric space group. The crystallographic problem encountered was one reason for performing DFT calculations on this compound. The results of the DFT calculations confirmed those of the structural analysis with some differences especially in the bond lengths between the metal and sulfur atoms (see Table 2). In general, the distances obtained from X-ray analysis are shorter than the calculated ones, with the only exception of the metal–oxo distances, which are slightly longer. With these two data sets (X-ray data and DFT data) for **3**, we are now able to discuss the structural parameters of compound **3** as well as of compound **2** with some certainty, despite the crystallographic problems concerning the structure of **3**.

In compound **2** the metal is pseudo-octahedrally coordinated. The thioethers form only very weak bonds, if at all, to the molybdenum atoms (interatomic distances: 2.931, 3.002 Å). The molybdenum atoms are positioned above (0.3647 and 0.3664 Å) the plane that consists of three alkox-

Table 2. Selected bond lengths and angles obtained from an X-ray structural analysis of $[\{MoO_2[O(CH_2)_2S(CH_2)_2O]\}_2]$ (**2**) and $[\{WO_2[O(CH_2)_2S(CH_2)_2O]\}_3]$ (**3**) and from DFT calculations for $[\{WO_2[O(CH_2)_2S(CH_2)_2O]\}_3]$ (**3**).

	$[\{MoO_2(OSO)\}_2]$ (**2**)[a] X-ray	$[\{WO_2(OSO)\}_3]$ (**3**)[a] X-ray	$[\{WO_2(OSO)\}_3]$ (**3**)[a] DFT
M=O [Å]	1.6916(19), 1.6912(19)	1.707(12)	1.7060
	1.6926(19), 1.6982(18)	1.712(11)	1.7062
		1.734(11)	1.7076
M–S [Å]	2.931(4), 3.002(5)	2.793(4), 2.812(4), 2.827(4),	3.1220, 3.1286, 3.2135
$M–O_{alkoxy}$ [Å]	1.8973(18)	1.865(10), 1.889(10)	1.9544, 2.0095
	1.8973(18)	1.888(10), 1.897(11)	1.9350, 1.9461
		1.862(10), 1.880(10)	1.9274, 1.9377
$M–O_{bridge}$	2.0718(17), 2.1410(17)	1.870(10), 1.944(8)	1.9206, 1.9407
	2.0940(17), 2.1484(18)	1.853(8), 1.937(7)	1.9112, 1.9358
		1.885(10), 1.905(10)	1.9143, 1.9487
O=M=O [°]	106.65(9), 108.19(10)		
$O_{bridge}–M–O_{bridge}$ [°]	70.04(7), 69.49(7)	85.2(4), 85.4(3), 84.9(4)	86.32, 86.11, 84.26
$M–O_{bridge}–M$ [°]	105.72(7), 106.24(7)	150.7(5), 153.7(5), 153.6(4)	139.693, 150.67, 151.89
$O_{alkoxy}–M–O_{alkoxy}$ [°]	90.34(7), 90.99(7)	90.5(4), 86.4(4), 94.1(4)	85.94, 86.91, 92.29
S–M=O [°]	167.52(7), 165.71(7)	172.7(4), 170.9(4), 170.3(4)	164.76, 164.22, 167.00
C–S–C [°]	100.70(13), 101.76(13)	100.9(8), 100.7(8), 101.1(8)	100.88, 102.20, 102.54

[a] OSO = $^{-}OC_2H_4SC_2H_4O^{-}$.

ylate groups and one oxo function in the direction of the second oxo ligand at each molybdenum atom, which is coordinated *trans* to the thioether sulfur. Within the Mo_2O_2 ring, the angles at the metal atom are smaller than 90°, whereas the angles at the oxygen atom are larger. The tridentate ligands and the oxo ligands that are coordinated *trans* to the sulfur atoms are positioned on different sides of the Mo_2O_2 ring. The two oxo functions, as well as the two tridentate ligands, are on the same side of this ring, although one could assume that the *trans* form would be sterically less demanding.

Compound **3** is analogous to the published tungsten trimer, but phenyl rings bridge the alkoxylate and thioether functions instead of ethyl groups.[24] In the published complex, two of the tridentate ligands and one oxo function are positioned on one side of the W1–W2–W3 plane, whereas the remaining two oxo functions and one tridentate ligand are on the opposite side. For compound **3**, all oxo functions are positioned on the same side of the W1–W2–W3 plane and all tridentate ligands on the opposite side. From the structural analysis, we obtained metal–oxo distances that were longer, and metal–sulfur and metal–oxygen distances that were shorter than the parameters obtained from DFT calculations. The significantly longer metal–sulfur distances in the theoretical investigations were also observed for compound **2** (compare Table 2 and Table 3). Therefore, we think that the structural analysis gives a more accurate value for this parameter than the DFT calculations. In compound **3**, the metal is again coordinated in a pseudo-octahedral geometry that is slightly less distorted than that of compound **2**. The tungsten–sulfur distances (2.79, 2.81, and 2.83 Å) are shorter than the molybdenum–sulfur distances in compound **2**. The oxo ligand is bound *trans* to the sulfur atom with a short distance of 1.71 to 1.73 Å. In this way, the ligand that is most tightly bound to tungsten is in a *trans* position to the ligand that is most weakly bound to the metal, which is the most stable geometry. All other metal–oxygen distances to the alkoxylate functions as well as to the bridging oxygen atoms are within the usual range of 1.86 to 1.95 Å for oxygen–tungsten single bonds. The tungsten atoms are positioned slightly above the equatorial plane (two bridging oxygen atoms, two alkoxylate functions) in the direction of the oxo ligands by 0.04 to 0.36 Å.

DFT Calculations

DFT calculations were not only performed to confirm the results of the X-ray crystal structure analysis for compound **3**, but also to understand the formation of surprisingly different complexes for molybdenum and tungsten with the same ligand and by the same preparation method. The most important differences between the two structures can be summarized shortly as follows: (i) a trimeric structure for the tungsten compound versus a dimeric structure for the molybdenum compound; (ii) former oxo ligands as bridging atoms for the tungsten compound versus alkoxylate functions of the thioether ligand for the molybdenum compound.

We performed calculations on both of the observed structures for the two metals in order to better understand the different behavior of molybdenum and tungsten regarding the formation of the two significantly different complexes. The important parameters obtained from DFT calculations are summarized in Table 3.

The most significant differences between the molybdenum and the tungsten compounds are as follows: The metal-to-bridging-oxygen distances for the trimer are much more unsymmetrical for the molybdenum than for the tungsten compound. It seems that the molybdenum center is somehow reluctant to share one of its oxo ligands with another molybdenum atom and to form a single bond instead of a double bond to the respective oxygen atom. The double-bond character of the metal–oxygen interaction is certainly more conserved in the molybdenum than in the tungsten trimer. In the dimer as well as in the trimer the molybdenum–oxo bonds are shorter than the tungsten–oxo bonds. All this is an indication that the molybdenum–oxo

Table 3. Selected bond lengths and angles obtained from DFT calculations for the molybdenum dimer **2** and trimer and for the tungsten dimer and trimer **3**.

	[{MoO_2(OSO)}$_2$] (**2**)[a]	[{MoO_2(OSO)}$_3$][a]	[{WO_2(OSO)}$_2$][a]	[{WO_2(OSO)}$_3$] (**3**)[a]
M=O [Å]	1.7127, 1.7295	1.6988	1.7189, 1.7344	1.7060
	1.7124, 1.7294	1.7014	1.7185, 1.7343	1.7078
		1.7035		1.7098
M–S [Å]	3.3557, 3.4079	3.1567/3.2187/3.2778	3.2903, 3.3594	3.1220, 3.1486, 3.2135
M–O_{alkoxy} [Å]	1.9227	1.9421, 1.9505	1.9116	1.9348, 1.9409
	1.9232	1.9411, 1.9561	1.9119	1.9333, 1.9445
		1.9299, 1.9410		1.9221, 1.9325
M–O_{bridge}	2.1265, 2.1363	1.8872/1.9723	2.1122, 2.1390	1.8988, 1.9453
	2.1273, 2.1349	1.8876/1.9710	2.1116, 2.1346	1.9010, 1.9441
		1.9168/1.9695		1.9295, 1.9440
O=M=O [°]	108.05, 108.09		107.22, 107.36	
O_{bridge}–M–O_{bridge} [°]	68.35, 68.39	86.76, 87.91, 93.68	67.87, 67.96	83.10, 85.88, 91.71
M–O_{bridge}–M [°]	110.26, 110.28	142.35, 150.89, 156.09	110.95, 111.10	142.99, 150.15, 155.62
S–M=O [°]	163.47, 164.36	163.79, 164.03, 166.84	163.27, 164.32	164.23, 164.76, 167.00
S–M–$O_{equatorial}$ [°]	76.32	77.46	68.45	77.73
C–S–C [°]	101.29, 101.33	100.75, 100.79, 102.26	101.15, 101.21	100.72, 100.95, 102.08
HOMO LUMO gap [eV]	0.144	0.127	0.175	0.157

[a] OSO = $^-OC_2H_4SC_2H_4O^-$.

bond is stronger than the tungsten–oxo bond, as would be expected when taking the hard–soft interactions into account.

The metal–sulfur distances provide a further clue to the differing behavior of the two metals in reaction with the same ligand. It has to be noted that, although these calculated parameters are the ones that differ most from the X-ray structural parameters, at least the trend seems to be represented correctly. The metal–sulfur distances for the dimer as well as for the trimer are shorter for the tungsten than for the molybdenum compound, and the metal–sulfur distances for the trimers are shorter than the distances for the dimers. The octahedral geometry is less distorted for the tungsten trimer than for the tungsten dimer, providing more space for the sixth ligand, the sulfur atom. Even though the metal–sulfur distances in all four cases are significantly longer than for a regular metal–thioether bond, the observed parameters show that the trimer provides a coordination geometry that enhances the formation of a metal–sulfur bond much more than the dimer does. We also have to keep in mind that the actual metal–sulfur distances, at least for the two compounds that were analyzed by X-ray diffraction, are much shorter than those provided by the DFT calculations. We conclude from all of this that molybdenum forms the dimeric structure, because it is able to keep both of the doubly bonded oxo ligands, and that tungsten forms the trimeric structure because it is able to form a stronger metal–sulfur interaction. This behavior is confirmed by the fact that with similar ligand sets, only a tungsten trimer,[24] where terminal oxo ligands are converted into bridging oxo ligands, and molybdenum monomers[22] and dimers,[25] where the oxo ligands are retained as doubly bonded, are obtained and structurally characterized.

Again, this shows that molybdenum forms stronger interactions with oxygen than tungsten but weaker interactions with sulfur.

Electrochemical Results

In order to evaluate the influence of the metal and of the ligand atoms (S versus Se) on the redox properties, compounds **2**, **3**, and **4** were investigated by differential pulse voltammetry (DPV). This method was chosen over cyclic voltammetry because all compounds, but especially compound **4**, were only slightly soluble in acetonitrile, and the signals of the redox processes in the cyclic voltammograms were rather weak (see Figure 4), whereas in the oxidative as well as in the reductive DPVs all transitions were sharp and sufficiently intense and therefore easily detected (Figure 5). The peak positions given in Table 4 were determined from both the reductive and the oxidative DPVs as an average. For each of the compounds [**2** (MoS), **3** (WS), **4** (WSe)], two reversible transitions were observed in the differential pulse voltammograms for the redox processes $M^{IV} \leftrightarrow M^{V}$ and $M^{V} \leftrightarrow M^{VI}$ (see Figure 4). As expected, the redox processes $M^{VI} \leftrightarrow M^{V}$ and $M^{V} \leftrightarrow M^{IV}$ for the molybdenum compound are at a higher voltage than those for the respective tungsten compound, and those for the tungsten–selenium compound are at a higher voltage than those for the tungsten–sulfur compound. A third redox process was found at a rather high voltage for all three compounds. It showed irreversible behavior in the cyclic voltammograms, but a slightly shifted transition was also observed in the reductive DPV (see Figure 5). This leads to the conclusion that the third redox process is due to a structural reorganization of the molecule, where the oxidation occurs much more readily than the reduction. Because the oxidation probably takes place at the sulfur/selenium atom, the metal–sulfur/metal–selenium bond must dissolve, and therefore a reorganization of the molecule is necessary. We assume that the reduction at the sulfur/selenium atom involves a more demanding structural reorganization than the oxidation process. Therefore, reduction occurs much more slowly, and it could not

Table 4. Redox potentials for the molybdenum and tungsten compounds with the tridentate thioether/selenoether alkoxylate ligands for the $M^{IV}\leftrightarrow M^{V}$ and $M^{V}\leftrightarrow M^{VI}$ transitions and for the oxidation at the ligand atom as obtained from DPV investigations referenced internally vs. ferrocene/ferrocenium.

Compound	$E_{1/2}$ $M^{IV}\leftrightarrow M^{V}$ vs. Fc/Fc^{+} [V]	$E_{1/2}$ $M^{V}\leftrightarrow M^{VI}$ vs. Fc/Fc^{+} [V]	$E_{1/2}$ ($[MO_2(OXO)]\leftrightarrow[MO_2(OXO)]^{+}$) vs. Fc/Fc^{+} [V]
$[\{MoO_2(OSO)\}_2]$ (**2**)[a]	–0.93	0.31	1.49
$[\{WO_2(OSO)\}_3]$ (**3**)[a]	–1.41	–0.07	1.24
$[\{WO_2(OSeO)_n\}$ (**4**)[b]	–1.37	–0.02	0.96

[a] OSO = $^{-}OC_2H_4SC_2H_4^{-}$. [b] OSeO = $^{-}OC_2H_4SeC_2H_4^{-}$.

be observed in the CV but in the much slower DPV recording. Interestingly, the third transition for compound **4** (WSe) is at a significantly lower voltage than the transition for compound **3** (WS), reversing the observed behavior for the two transitions taking place at the metal atom with more positive potentials for **4** (WSe) than for **3** (WS). This is another indication that this redox process does indeed take place at the ligand atom. Here, the oxidation of selenium is easier to achieve than that of sulfur, as would be expected by taking the sizes of the two atoms and the metallic character of the selenium atom into account.

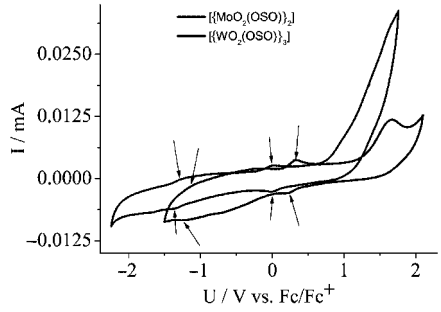

Figure 4. Cyclic voltammograms of compounds $[\{MoO_2[O(CH_2)_2S(CH_2)_2O]\}_2]$ (**2**) and $[\{WO_2[O(CH_2)_2S(CH_2)_2O]\}_3]$ (**3**) referenced vs. ferrocene/ferrocenium showing two reversible redox processes (indicated by arrows) and an irreversible oxidation (of very poor intensity for **3**). The current values of **3** were multiplied by a factor of 4 in order to fit all the data into one graph.

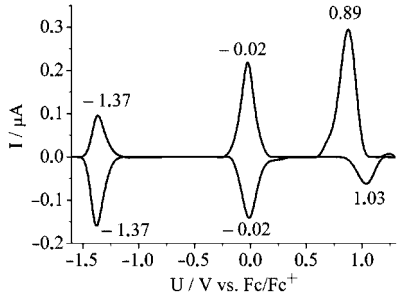

Figure 5. Reductive and oxidative differential pulse voltammograms of compound **4** referenced vs. ferrocene/ferrocenium. The plots were generated using the automatic baseline correction function of the Gepris software.

The redox potentials of compounds MoO_2Cl_2(dme),[18] WO_2Cl_2(dme),[19] $MoO_2Cl_2[MeS(CH_2)_2SMe]$,[14] and $WO_2Cl_2[MeS(CH_2)_2SMe]$ (**1**) were also compared (see Table 5). Here, we used cyclic voltammetry and observed quasi-reversible behavior for all compounds for the $M^{V}\leftrightarrow M^{VI}$ transition. In the range –1.0 to –1.5 V, an irreversible reduction occurs in all cases probably because of the loss of one oxo ligand accompanying the reduction to M^{IV}. The formation of this new species led to the emergence of new signals in the voltammograms. We therefore only compared the potentials of the quasi-reversible process assigned to the $M^{V}\leftrightarrow M^{VI}$ transition. Figures showing a long-range cyclic voltammogram (including the irreversible reduction and ligand-centered quasi-reversible oxidation) of MoO_2Cl_2(dme), a short-range cyclic voltammogram of $MoO_2Cl_2(MeSC_2H_4SMe)$, and a long-range cyclic voltammogram of WO_2Cl_2(dme) with the internal reference ferrocene can be found in the Supporting Information.

Table 5. Redox potentials for the molybdenum and tungsten compounds with the bidentate ether/thioether ligands for the $M^{V}\leftrightarrow M^{VI}$ redox processes referenced internally vs. ferrocene/ferrocenium.

Compound	$E_{1/2}$ $M^{V}\leftrightarrow M^{VI}$ vs. Fc/Fc^{+} [V]
MoO_2Cl_2(dme)	–0.17
$MoO_2Cl_2(MeSC_2H_4SMe)$	–0.15
WO_2Cl_2(dme)	–0.34
$WO_2Cl_2(MeSC_2H_4SMe)$ (**1**)	–0.28

Again, the molybdenum compounds have potentials that are higher than their tungsten analogs, and the complexes with sulfur ligand atoms have potentials that are higher than their counterparts with oxygen ligand atoms. The latter differences are again smaller (between 20 and 60 mV) than the differences between molybdenum and tungsten compounds, which are about three times larger (between 130 and 170 mV). Since the bonds between metal and sulfur atoms exhibit π–π-interactions, it can be noted that the differences between the redox potentials of the molybdenum and tungsten thioether complexes are smaller than those between the complexes with the oxygen ligand atoms.

Again, changing the metal atoms has a much more significant influence on the redox potentials than changing the ligand atoms.

Concluding Remarks

We have seen that molybdenum and tungsten form almost identical complexes with the bidentate ether and thioether ligands. The metal atom does not affect the structure of the complexes, though it has an influence on the stability of the complexes because of a difference in the strength of orbital overlap. For the oxygen-atom-transfer enzymes, where only mono- or bidentate ligands are present, a geo-

metrical or steric influence as a result of changing the metal atom can be excluded.

Changing the ligand atoms does not result in any significant structural alterations, with the only exception of the metal-to-ether/thioether-ligand-atom bond length and angle, but these differences are merely a result of the different radii of the ligand atoms. There was no indication of a significant electronic influence of changing the ligand atoms (oxygen versus sulfur) on the metal, except that the potentials of the molybdenum and tungsten complexes were closer together with sulfur ligation than with oxygen ligation.

With the tridentate bisanionic ligands, molybdenum and tungsten form rather different complexes, the former giving a dimeric and the latter a trimeric complex. Interestingly, the thioether function forms no explicit bond with the molydenum, whereas the analogous ether ligand does form a bond with this metal atom (no analogous compound was published for tungsten).[22]

We conclude from this that the structural influence of the ligand atom plays a vital role in structurally demanding ligands (tridentate) but not in those with a simpler geometry (bidentate or monodentate).

This may be because the hard–soft interactions between the ether/thioether function of the ligands and the metal center favor the oxygen–molybdenum combination over the sulfur–molybdenum combination. Molybdenum prefers O-functional ligands although it has been said that the bond strength of ether functions to metals increases within the group of the chalcogens.[21] Interestingly, in nature the ligand–metal combinations that are less favorable than others from this point of view occur at the active sites of the OATs: for instance the coordination of thiolate (cysteine) to molybdenum at the active site of the DMSO reductase of *Desulfovibrio desulfuricans*[8] or the coordination of serine to tungsten in the aldehyde oxidoreductase of *Pyrococcus furiosus*.[11]

The influence of the metal on the redox potential is, as expected, such that the molybdenum complexes have more positive redox potentials than the analogous tungsten complexes in all cases. With regard to the enzymes, this means that in all cases one metal is better suited for the catalyzed reaction with the substrate, while with the other metal the active site is more easily regenerated. For a given enzyme, there is always an advantage as well as a disadvantage in using either of the two metals, molybdenum or tungsten. If the redox potential is important for the choice of the metal, the basis of this choice would be a difference in the redox behavior of the two metals at different temperatures[26] rather than their relative redox potentials at room temperature.

The influence of the ligand atoms on the redox potentials is small but of consequence; the sulfur ligands cause more positive redox potentials than the oxygen ligands, and the selenium ligands cause more positive potentials than the sulfur ligands. However, the observed differences are smaller than those that result from changing the metal atoms.

The fact that there are two molybdenum cofactors that both catalyze the reduction of DMSO but contain molybdenum coordinated to cysteine in one case (*Desulfovibrio desulfuricans*)[8] and to serine in the other case (*Rhodobacter spharoides*)[7a,7b] is another indication that the use of different amino acids as ligands to the active sites is probably not an answer to the substrate demands on the redox potentials of the enzymes.

In addition, there does not seem to be any correspondence between the atom that is oxidized or reduced and the coordinated amino acid. Carbon can be oxidized by active sites that have selenocysteine (formate dehydrogenase from *E. coli*) or serine (aldehyde oxidoreductase from *P. furiosus*)[11] coordination. As mentioned above, sulfur can be oxidized by active sites that have serine or cysteine coordination, and nitrogen can be reduced by active sites that have cysteine (nitrate reductase from *E. coli*)[27] or aspartate (nitrate reductase from *Paracoccus pantotrophus*)[10] coordination, to name only a few examples.

The only parameters that are significantly influenced by changing the ligand atoms and which are not compromised by being part of a multidentate ligand system within the enzymes are the length and the strength of the metal–amino acid bond. If there is a reason for using different amino acid ligands, it is probably the ability to stabilize the active-site–substrate complex during turnover of the enzymatic reaction in cooperation with the peptide side chain residues close to the active site. A substantial effect of the coordinated amino acid on the enzymatic reaction by itself seems to be unlikely.

To finally answer the question about the reason for using different amino acid ligands at the active sites of the OATs, two strategies are to be followed. One is to synthesize model compounds for the enzyme–substrate complexes and to evaluate the ability of different amino acid ligands to stabilize these complexes with different substrates. The other is to undertake theoretical investigations of the intermediate states of the active sites, taking into account the influence of the peptide side chain on the stabilizing effect of the coordinated amino acid. These are challenging tasks for the future.

Experimental Section

Materials: $MoO_2Cl_2(dme)$,[18] $WO_2Cl_2(dme)$,[19] $MoO_2Cl_2[MeS(CH_2)_2SMe]$,[14] $WOCl_4$,[28] $Me(SCH_2CH_2S)Me$,[29] $WO_2(acac)_2$[30] and bis(2-hydroxyethyl)selenide[31] were prepared as described in the literature. $MoO_2(acac)_2$ and bis(2-hydroxyethyl) sulfide are commercially available and were used as received. Reagent-grade solvents were dried and distilled prior to use. All manipulations were performed under dry and oxygen-free conditions in nitrogen using Schlenk line techniques.

Syntheses

$WO_2Cl_2(MeSCH_2CH_2SMe)$ (1): Liquid $(Me_3Si)_2O$ (0.341 g, 2.10 mmol) was added to a suspension of freshly sublimed $WOCl_4$ (0.68 g, 2.00 mmol) in CH_2Cl_2 (20 mL). The orange crystals were

slowly consumed to give a yellow solution. After stirring for approximately 1.5 h at room temp., a light yellow solid precipitate was obtained. A solution of $MeSCH_2CH_2SMe$ (0.366 g, 3.00 mmol) in CH_2Cl_2 (10 mL) was added, and the reaction mixture was stirred overnight and filtered to remove the brownish precipitate. The clear yellow filtrate was concentrated at room temp. in vacuo until the solid began to precipitate. After keeping this solution at 4 °C overnight colorless crystals were obtained. The crystals were collected on a filter, washed once with diethyl ether (5 mL), and dried in vacuo. Yield: 0.53 g, 65%. M.p. 128–130 °C. $C_4H_{10}Cl_2S_2O_2W$ (407.90): calcd. C 11.75, H 2.46; found C 11.95, H 2.54. IR (KBr): $\tilde{\nu}$ = 3013 (m), 2966 (m), 2933 (m), 1868 (w), 1618 (w), 1424 (m), 1326 (w), 1259 (s), 1179 (w), 1145 (w), 1099 (m), 1028 (m), 956 (vs), 917 (vs), 883 (s), 841 (s), 803 (s), 646 (s), 444 (w), 363 (m), 344 (vs) cm^{-1}. EI-MS (70 eV): *m/z* (%) = 409 (1) $[M^+]$, 288 (100) $[WO_2Cl_2]^+$, 251 (49) $[WO_2Cl]^+$, 255 (12) $[WCl_2]^+$.

$[\{MoO_2[O(CH_2)_2S(CH_2)_2O]\}_2]$ (2): Bis(2-hydroxyethyl) sulfide (0.25 g, 2.05 mmol) was added to a stirred solution of $MoO_2(acac)_2$ (0.65 g, 2.00 mmol) in CH_2Cl_2 (20 mL) at room temp. The reaction mixture was stirred for 24 h. A small amount of white precipitate was filtered off, and the solvent was removed in vacuo. The residue was extracted with *n*-hexane (20 mL) and stored at room temp. for several days to yield colorless crystals. Yield: 0.10 g, 41%. M.p. 190 °C. $C_8H_{16}O_8S_2Mo_2$ (499.84): calcd. C 19.36, H 3.25; found C 19.61, H 3.26. IR (KBr): $\tilde{\nu}$ = 1460 (m) 1415 (m), 1403 (m), 1368 (s), 1305 (w), 1277 (m), 1263 (m), 1218 (w), 1181 (w), 1069 (s, $\nu_{Mo=O}$), 1041 (s), 1025 (s), 997 (m), 936 (m), 910 (m), 802 (s), 723 (m), 694 (w), 651 (w), 571 (m), 530 (m), 475 (m), 396 (m), 360 (s) cm^{-1}. ^{1}HNMR ($CDCl_3$, 200 MHz): δ = 2.31 (t), 3.36 (t) ppm. EI-MS (70 eV): *m/z* (%) = 248 (11) $[\{MoO_2[O(CH_2)_2S(CH_2)_2O]\}^+]$, 216 (40) $[\{Mo[O(CH_2)_2S(CH_2)_2O]\}^+]$.

$[\{WO_2[O(CH_2)_2S(CH_2)_2O]\}_3]$ (3): Bis(2-hydroxyethyl) sulfide (0.12 g, 1.00 mmol) was added to a stirred solution of $WO_2(acac)_2$ (0.41 g, 1.00 mmol) in CH_2Cl_2 (20 mL) at room temp. The reaction mixture was stirred for 24 h. The white precipitate was filtered off, and the clear filtrate was concentrated under reduced pressure until the solution was saturated. The solution was stored overnight at room temp. to yield colorless crystals. Yield: 0.11 g, 32%. M.p. 240 °C (dec.). $C_{12}H_{24}O_{12}S_3W_3$ (1007.90): calcd. C 14.30, H 2.40; found C 14.51, H 2.50. IR (KBr): $\tilde{\nu}$ = 1464 (vs), 1378 (vs), 1306 (w), 1262 (w),1261 (w), 1170 (w),1153 (w),1091 (m), 1066 (m, $\nu_{W=O}$), 1033 (m), 962 (w), 935 (w), 858 (w), 838 (w), 801 (m), 722 (m), 657 (w) cm^{-1}. EI-MS (70 eV): *m/z* (%) = 352 (33) $[\{WO_3[O(CH_2)_2S(CH_2)_2O]\}^+]$, 337 (100) $[\{WO_2[O(CH_2)_2S(CH_2)_2O]\}^+]$.

$[\{WO_2[O(CH_2)_2Se(CH_2)_2O]\}_n]$ (4): A solution of bis(2-hydroxyethyl)selenide (0.17 g, 1.00 mmol) in CH_2Cl_2 (5 mL) was added to a stirred solution of $WO_2(acac)_2$ (0.41 g, 1.00 mmol) in CH_2Cl_2 (20 mL) at room temp. The reaction mixture was stirred for 2 d. The green solution turned yellow, and a small amount of yellow precipitate formed. The precipitate was filtered off, and ether was added to the filtrate to precipitate the product. The yellow product was collected by filtration and washed with diethyl ether twice. The compound was dried in vacuo. Yield: 0.23 g, 60%. M.p. 210 °C. $C_4H_8O_4SeW$ (383.91): calcd. C 12.55, H 2.11; found C 12.63, H 2.18. IR (KBr): $\tilde{\nu}$ = 1527 (w), 1459 (m), 1400 (m), 1377 (m), 1261 (vs), 1094 (vs, $\nu_{W=O}$), 1020 (vs), 962 (w), 939 (w), 863 (w), 800 (vs), 722 (w), 703 (w), 668 (w), 583 (w), 533 (w), 472 (w) cm^{-1}. ^{1}HNMR ([D$_6$]DMSO, 300 MHz): δ = 2.60 (t), 3.56 (t) ppm. ^{13}CNMR ([D$_6$]-DMSO, 300 MHz): δ = 26.14 (s), 61.62 (s) ppm. ^{77}Se NMR ([D$_6$]-DMSO, 500 MHz): δ = 100.22 (s) ppm. EI-MS (70 eV): *m/z* (%) = 355 (50) $[M^+ - CH_2CH_2]$.

Electrochemistry

Electrochemical measurements were performed with an AUTOLAB PGSTAT12 potentiostat/galvanostat with a glassy carbon working electrode, a platinum wire reference electrode, and a platinum wire auxiliary electrode, in acetonitrile solutions within a glove box under argon. The supporting electrolyte was Bu_4NPF_6 (0.1 M) used as received from Fluka. Acetonitrile used for the electrochemistry was predried with $CaCl_2$, dried by reflux over CaH_2 for 2 d, and distilled onto freshly regenerated molecular sieves A3. Referencing was done internally using the ferrocene/ferrocenium couple. The temperature during the measurements was controlled with a Julabo refrigerated/heating circulator FP50-MV at 25 °C. The solutions were prepared within a glove box by dissolving the Bu_4NPF_6 electrolyte (10^{-3} mol) and the compounds (10^{-6} mol) in acetonitrile (10 mL) to give 10^{-4} M solutions. For reasons of poor solubility, compound **4** could only be prepared as an approximately 0.5×10^{-5} M solution.

Other Physical Measurements

Melting points were obtained in sealed capillaries with a Büchi B 540 instrument and were not corrected. Elemental analyses were performed with a Heraeus CHN-O-Rapid elemental analyzer. Infrared spectra were recorded as KBr pellets with a Bio-Rad Digilab FTS-7 spectrometer from 4000 to 300 cm^{-1}. NMR spectra were recorded with Bruker Avance 200, AM 300 and Bruker Avance 500 NMR spectrometers and referenced to the chemical shifts of the deuterated solvent. All NMR-grade solvents were dried prior to use. The chemical shifts are reported in ppm; external reference $SiMe_4$ for ^{1}H and ^{13}C nuclei, and $SeMe_2$ for ^{77}Se nuclei. Mass spectra were obtained with a Finnigan MAT system 8230 or Varian MAT CH5 instrument by EI-MS methods.

X-ray Crystallography

Data for crystal structures of compounds **1**, **2**, and **3** were collected with a Stoe–Siemens–Huber four-circle diffractometer coupled to a Siemens CCD area detector with graphite-monochromated Mo-K_α radiation (λ = 0.71073 Å). All structures were solved by direct methods (SHELXS-97)[32] and refined with all data by full-matrix least-squares methods on F^2.[33] All non-hydrogen atoms were refined anisotropically. The hydrogen atoms were included at geometrically calculated positions and refined using a riding model. Parameters of the X-ray crystallography are summarized in Table 6. CCDC-280029 (**1**), CCDC-280030 (**2**), and CCDC-280028 (**3**) contain the supplementary crystallographic data for this paper. These data can be obtained free of charge from The Cambridge Crystallographic Data Centre via www.ccdc.cam.ac.uk/data_request/cif.

DFT Calculations

All calculations have been carried out with the Gaussian G03[34] program package using the implemented DFT variant B3LYP[35,36] (Becke three-parameter exchange functional B3 and the Lee–Yang–Parr correlation functional LYP). A basis consisting of the well-established small core ECP[37] (for Mo and W), 3-21g[38] (for carbon and hydrogen) and following a proposal by K. Peterson,[39,40] a modified 6-31G basis including double diffuse functions [6-31G(d′, p′)] to give a suitable description of the lone pairs on oxygen and sulfur were used.

All structures were fully optimized without employing any symmetry constraints. The starting geometries were taken from experimental data. Analytical frequency calculations were performed to verify these structures as local minima.

Supporting Information (see footnote on the first page of this article): Cyclic voltammograms of MoO_2Cl_2(dme), MoO_2-

Table 6. Crystallographic parameters.

	$WO_2Cl_2(MeSC_2H_4SMe)$ (**1**)	$[\{MoO_2(OSO)\}_2]$ (**2**)[a]	$[\{WO_2(OSO)\}_3]\cdot CH_2Cl_2$ (**3**)[a]
Formula	$C_4H_{10}Cl_2O_2S_2W$	$C_8H_{16}Mo_2O_8S_2$	$C_{13}H_{25}Cl_2O_{12}S_3W_3$
M [g/mol]	408.99	496.21	1091.96
Crystal system	hexagonal	monoclinic	monoclinic
Space group	$P6(5)$	$P21/n$	$P2(1)$
a [Å]	7.3222(3)	9.4839(7)	11.615(2)
b [Å]	7.3222(3)	12.4405(7)	7.8739(16)
c [Å]	33.3889(17)	12.8003(7)	14.4620(3)
α [°]	90	90	90
β [°]	90	101.567(4)	111.81(3)
γ [°]	120	90	90
V [Å^3]	1550.30(12)	1479.56(14)	1228.0(4)
Z	6	4	2
μ [cm^{-1}]	120.5	20.08	145.45
Reflections collected	15469	22121	12796
Independent reflections	1757	2554	4153
Completeness of θ [°]	99.4% (24.80°)	99.7% (24.84°)	97.6% (24.94°)
$R_1[I_0 > 2\sigma(I_0)]$	0.0247	0.0180	0.0350
$wR_2[I_0 > 2\sigma(I_0)]$	0.0535	0.0442	0.0904
R_1[all data]	0.0260	0.0228	0.0403
wR_2[all data]	0.0538	0.0451	0.0957

$R_1 = \Sigma||F_o| - |F_c||/\Sigma|F_o|$; $wR_2 = [\Sigma_w(F_o^2 - F_c^2)^2/\Sigma wF_{oi}^4]^{1/2}$

[a] (OSO) = $^-OC_2H_4SC_2H_4O^-$.

$Cl_2(MeSC_2H_4SMe)$ and WO_2Cl_2(dme), and the complete list of data obtained from DFT calculations.

Acknowledgments

Financial support from the Institut für Anorganische Chemie, University Goettingen, is gratefully acknowledged.

[1] J. H. Enemark, J. J. A. Cooney, *Chem. Rev.* **2004**, *104*, 1175–1200.
[2] M. K. Johnson, D. C. Rees, M. W. W. Adams, *Chem. Rev.* **1996**, *96*, 2817–2840, DOI: 10.1021/cr950063d.
[3] S. K. Das, D. Biswas, R. Maiti, S. Sarkar, *J. Am. Chem. Soc.* **1996**, *118*, 1387–1397, DOI: 10.1021/ja9511580.
[4] J. Bernholc, E. I. Stiefel, *Inorg. Chem.* **1985**, *24*, 1323–1330.
[5] H. Oku, N. Ueyama, A. Nakamura, *Chem. Lett.* **1996**, 1131–1132.
[6] R. Hille, *Chem. Rev.* **1996**, *96*, 2757–2816, DOI: 10.1021/cr950061t.
[7] a) H. Schindelin, C. Kisker, J. Hilton, K. V. Rajagopalan, D. C. Rees, *Science* **1996**, *272*, 1615–1621; b) G. N. George, J. Hilton, K. V. Rajagopalan, *J. Am. Chem. Soc.* **1996**, *118*, 1113–1117; c) G. N. George, J. Hilton, C. Temple, R. C. Prince, K. V. Rajagopalan, *J. Am. Chem. Soc.* **1999**, *121*, 1256–1266.
[8] J. M. Dias, M. E. Than, A. Humm, R. Huber, G. P. Bourenkov, H. D. Bartunik, S. Bursakov, J. Calvete, J. Caldeira, C. Carveiro, J. J. G. Moura, I. Moura, M. J. Romão, *Structure* **1999**, *7*, 65–79.
[9] J. C. Boyington, V. N. Gladyshev, S. V. Khangulov, T. C. Stadtman, P. D. Sun, *Science* **1997**, *275*, 1305–1308.
[10] M. G. Bertero, R. A. Rothery, M. Palak, C. Hou, D. Lim, F. Blasco, J. H. Weiner, N. C. J. Strynadka, *Nat. Struct. Mol. Biol.* **2003**, *10*, 681–687.
[11] a) M. K. Chan, S. Mukund, A. Kletzin, M. W. W. Adams, D. C. Rees, *Science* **1995**, *267*, 1463–1469; b) Y. Hu, S. Faham, R. Roy, M. W. W. Adams, D. C. Rees, *J. Mol. Biol.* **1999**, *286*, 899–914.
[12] a) H. Raaijmakers, S. Maciera, J. M. Dias, S. Texeira, S. Bursakov, R. Huber, J. J. G. Moura, I. Moura, M. J. Romão, *Structure* **2002**, *10*, 1261–1272; b) H. Raaijmakers, S. Texeira, J. M. Dias, M. J. Almendra, C. D. Brondino, I. Moura, J. J. G. Moura, M. J. Romão, *J. Biol. Inorg. Chem.* **2001**, *6*, 398–404.
[13] R. Hart, W. Levason, B. Patel, G. Reid, *J. Chem. Soc., Dalton Trans.* **2002**, 3153–3159.
[14] M. D. Brown, M. B. Hursthouse, W. Levason, R. Ratnani, G. Reid, *Dalton Trans.* **2004**, 2487–2491.
[15] D. Sevdic, L. Fekete, *Inorg. Chim. Acta* **1982**, *57*, 111–117.
[16] P. M. Boorman, M. Islip, M. M. Reimer, K. J. Reimer, *J. Chem. Soc., Dalton Trans.* **1972**, 890–893.
[17] P. Berges, W. Hinrichs, A. Holzmann, J. Wiese, G. Klar, *J. Chem. Research (S)* **1986**, 10–11.
[18] B. Kamenar, M. Penavić, B. Kopar-Ćolig, B. Marković, *Inorg. Chim. Acta* **1982**, *65*, L245–L247.
[19] K. Dreisch, C. Andersson, C. Stålhandske, *Polyhedron* **1991**, *10*, 2417–2421.
[20] E. G. Hope, W. Levason, *Coord. Chem. Rev.* **1993**, *122*, 109–170.
[21] S. G. Murray, F. H. Hartley, *Chem. Rev.* **1981**, *81*, 365–414.
[22] A. J. Wilson, B. R. Penfold, C. J. Wilkins, *Acta Crystallogr. C: Cryst. Struct. Commun.* **1983**, *39*, 329–330.
[23] H. Müller, A. Holzmann, W. Hinrichs, G. Z. Klar, *Z. Naturforsch. Teil B* **1982**, *37*, 341–347.
[24] P. Berges, W. Hinrichs, A. Holzmann, J. Wiese, G. Klar, *J. Chem. Research (S)* **1986**, 10–11.
[25] V. McKee, C. J. Wilkins, *J. Chem. Soc., Dalton Trans.* **1987**, 523–528.
[26] C. Schulzke, *Dalton Trans.* **2005**, 713–720.
[27] C. S. Butler, J. M. Charnock, C. D. Garner, A. J. Thomson, S. J. Ferguson, B. C. Berks, D. J. Richardson, *Biochem. J.* **2000**, *352*, 859–864.
[28] V. C. Gibson, T. P. Kee, A. Shaw, *Polyhedron* **1990**, *9*, 2293–2298.
[29] O. V. Alekminskaya, N. V. Russavskaya, N. A. Korchevin, E. N. Deryagina, *Russ. J. Gen. Chem.* **2002**, *72*, 75–78.
[30] S.-B. Yu, R. H. Holm, *Inorg. Chem.* **1989**, *28*, 4385–4391.
[31] X. Hu, Z. Tian, Y. Chen, X. Lu, *Synth. Commun.* **2000**, *30*, 523–529.
[32] SHELXS-97, Programs for Structure Solution: G. M. Sheldrick, *Acta Crystallogr., Sect. A* **1990**, *46*, 467–473.
[33] G. M. Sheldrick, *SHELXL-97, Programs for Crystal Structure Refinement*, University of Göttingen, Germany, **1997**.

[34] M. J. Frisch, G. W. Trucks, H. B. Schlegel, G. E. Scuseria, M. A. Robb, J. R. Cheeseman, J. A. Montgomery, Jr., T. Vreven, K. N. Kudin, J. C. Burant, J. M. Millam, S. S. Iyengar, J. Tomasi, V. Barone, B. Mennucci, M. Cossi, G. Scalmani, N. Rega, G. A. Petersson, H. Nakatsuji, M. Hada, M. Ehara, K. Toyota, R. Fukuda, J. Hasegawa, M. Ishida, T. Nakajima, Y. Honda, O. Kitao, H. Nakai, M. Klene, X. Li, J. E. Knox, H. P. Hratchian, J. B. Cross, C. Adamo, J. Jaramillo, R. Gomperts, R. E. Stratmann, O. Yazyev, A. J. Austin, R. Cammi, C. Pomelli, J. W. Ochterski, P. Y. Ayala, K. Morokuma, G. A. Voth, P. Salvador, J. J. Dannenberg, V. G. Zakrzewski, S. Dapprich, A. D. Daniels, M. C. Strain, O. Farkas, D. K. Malick, A. D. Rabuck, K. Raghavachari, J. B. Foresman, J. V. Ortiz, Q. Cui, A. G. Baboul, S. Clifford, J. Cioslowski, B. B. Stefanov, G. Liu, A. Liashenko, P. Piskorz, I. Komaromi, R. L. Martin, D. J. Fox, T. Keith, M. A. Al-Laham, C. Y. Peng, A. Nanayakkara, M. Challacombe, P. M. W. Gill, B. Johnson, W. Chen, M. W. Wong, C. Gonzalez, and J. A. Pople, *Gaussian 03, Revision B.04*, Gaussian, Inc., Pittsburgh, PA, **2003**.
[35] C. Lee, W. Yang, R. G. Parr, *Phys. Rev. B* **1988**, *37*, 785–789.
[36] B. Miehlich, A. Savin, H. Stoll, H. Preuss, *Chem. Phys. Lett.* **1989**, *157*, 200–206.
[37] T. R. Cundari, W. J. Stevens, *J. Chem. Phys.* **1993**, *98*, 5555–5565.
[38] K. D. Dobbs, W. J. Hehre, *J. Comput. Chem.* **1987**, *8*, 880–893.
[39] G. A. Petersson, M. A. Al-Laham, *J. Chem. Phys.* **1991**, *94*, 6081–6090.
[40] G. A. Petersson, A. Bennett, T. G. Tensfeldt, M. A. Al-Laham, W. A. Shirley, J. Mantzaris, *J. Chem. Phys.* **1988**, *89*, 2193–2218.

Received: August 3, 2005
Published Online: December 9, 2005

